Glutamate Signaling, Associated With Satellite Glial Cells That Envelop Small Trigeminal Ganglion Neurons Is Highly Involved in the Neuropathic Pain

Yi Sul Cho
Kyungpook National University
Hyoung-Gon Ko
Kyungpook National University
Won Mah
University of North Carolina
Yu Shin Kim
Translational Sciences, University of Texas Health Science Center at San Antonio
Jin Young Bae
Kyungpook National University
Dong Ho Youn
Kyungpook National University
Dong Kuk Ahn
Kyungpook National University
Yong Chul Bae (ycbae@knu.ac.kr)
Kyungpook National University

Research Article

Keywords: Glutamate signaling, satellite glial cells (SGCs), small trigeminal ganglion, neuropathic pain

Posted Date: April 26th, 2021

DOI: https://doi.org/10.21203/rs.3.rs-445113/v1

Abstract

Recent studies implicate glutamate release from satellite glial cells (SGCs) surrounding the primary sensory neurons in the mechanisms of pathologic pain. However, little is known about the population of SGCs in the trigeminal ganglion that is involved in glutamate signaling associated with craniofacial neuropathic pain. To address this issue, we used quantitative analysis of electron microscopic immunogold labeling to investigate the changes in glutamate levels in trigeminal neurons and their enveloping SGCs in a rat model of craniofacial neuropathic pain, chronic constriction injury of inferior alveolar nerve (CCI-ION). The density of immunogold, a measure for glutamate concentration, in the neuronal cell bodies of all sizes, and in the SGCs surrounding them, was significantly higher in rats with CCI-ION than in sham-operated rats. This effect was more pronounced for the small neurons (2.2 times higher) and their SGCs (1.8 times higher) than for the medium and the large neurons and their SGCs, respectively. These findings suggest that each populations of SGCs and their surrounding trigeminal neurons of different type are involved in the glutamate signaling associated with neuropathic pain at a different level.

Introduction

The results of several recent studies suggest that satellite glial cells (SGCs) that envelop the cell bodies of the primary sensory neurons in the dorsal root ganglia (DRG) and the trigeminal ganglion (TG), play a crucial role in neuronal sensitization and pathologic pain[1,2]. The mechanism is thought to involve a reciprocal signaling between neurons and their enveloping SGCs, and between SGCs in the DRG and TG, i.e., SGCs, activated under pathologic conditions, release glutamate, cytokines and ATP, which act on neurons that they envelop, and on adjacent SGCs, thus contributing to augmentation of neuronal excitability and pathologic pain[1,3,4,5,6,7,8].

Primary sensory neurons and their enveloping SGCs form a morphologically- and functionally-distinct unit[9]. SGCs fall into 3 categories, according to the type of neuron that they envelop, small (C fiber) neurons, medium (Aδ fiber) neurons, and large (Aβ fiber) neurons[10]. In addition, SGCs that envelop large light neurons in the DRG have different morphological and functional features than those that envelop small dark neurons[11], suggesting that the SGCs that envelop different neuronal types may show different response to peripheral nerve injury. However, little is yet known about the various populations of SGCs and their differences in the context of pathologic pain. To provide more information on the SGCs and the primary sensory neurons in the TG that are involved in the pathologic pain, we here used electron microscopic immunogold labeling for glutamate and quantitative analysis of glutamate labeling in a rat model of craniofacial neuropathic pain, chronic constriction injury of the infraorbital nerve (CCI-ION).

Results

Rats with chronic constriction injury of the infraorbital nerve manifested mechanical allodynia

The air puff threshold for the area innervated by the infraorbital nerve (whisker pad) was significantly lower in rats with chronic constriction injury of the infraorbital nerve (CCI-ION) than controls on day 1 after surgery, and persisted until day 14, when the material used for electron microscopic analysis was harvested (Fig. 1).

Small neurons and their enveloping SGCs exhibited highly elevated levels of glutamate following CCI-ION

At EM, SGCs were easily distinguished from the neuronal somata they envelope by their electron-dense cytoplasm. Gold particles were dense in the cytoplasm of both neurons and SGCs and few in the extracellular matrix (Fig. 2). In neurons of all sizes, the density of gold particles was significantly higher after CCI-ION than sham group; this difference was larger for the small neurons than medium-sized and large neurons (130% higher in small, 67% in medium, and 44% in large neurons; Fig. 3A). Also, in SGCs that envelop neurons of all sizes, the density of gold particles was significantly higher after CCI-ION than sham; this difference was also higher for the SGCs that envelop small neurons than medium-sized and large neurons (110% higher in SGCs that envelop small neurons, 51% in SGCs that envelop medium neurons, and 46% in SGCs that envelop large neurons; Fig. 3B). The degree of positive correlation between the gold particle density in neurons and in their SGCs was also higher in CCI-ION rats than sham-operated rats (Fig. 4).

Discussion

The present study revealed that glutamate is increased significantly in trigeminal neurons of all sizes and their enveloping SGCs, but predominantly in small neurons and their SGCs, in a model of neuropathic pain associated with peripheral nerve injury. This suggests that each populations of satellite glial cells (SGCs) and their surrounding trigeminal neurons of different type are involved in the glutamate signaling associated with neuropathic pain at a different level.

Ever since the elegant studies by the Ottersen's group with postembedding immunogold showed that the density of gold particles coding for glutamate is linearly correlated with the concentration of glutamate in the brain[12,13], we, among others, have routinely used immunogold labeling as a reliable method for a semiquantitative estimation of level of glutamate as a signal substance in the neural tissue[14,15]. In the present study, we employed this method to evaluate changes in the levels of glutamate in trigeminal neurons and their enveloping SGCs in a model of neuropathic pain following peripheral nerve injury.

That the levels of glutamate in trigeminal neurons of all sizes were higher in rats with CCI-ION than in sham-operated rats is consistent with the results of previous light microscopic immunohistochemical studies in the DRG and TG neurons following peripheral nerve injury and inflammation[16,17]. Since there is

a positive correlation between the size of DRG neurons and the conduction velocity of their fibers[18,19], it is now widely accepted that the small, medium-sized, and large neurons in the DRG are roughly equivalent to neurons with C, Aδ, and Aβ fibers, respectively. Our results, then, support the idea that the release of glutamate from sensory fibers of all types is increased following CCI-ION[16,20,21,22], potentially leading to an increase in the excitability of their postsynaptic neurons in the superficial laminae (by C and Aδ fibers) as well as in the deep laminae (by Aβ fibers) of the spinal and medullary dorsal horn[23,24], which may further contribute to the development of pathologic pain.

The increase in the levels of glutamate following CCI-ION was the highest in small neurons (1.9 and 3.0 times higher than in medium-sized and in large neurons, respectively). This supports the notion that peripheral nerve injury leads to increased synaptic transmission primarily by central C fibers. Also, the increased synaptic transmission at the central synapses of C fibers in the superficial lamina of the medullary dorsal horn may cause more robust sensitization of their (nociceptive) postsynaptic neurons, compared to the A fiber synapses and their (non-nociceptive) postsynaptic neurons in the deep laminae of Vc. On the other hand, the synaptic facilitation of A fiber synapses in the deep laminae may also contribute to activation of nociceptive neurons in the superficial laminae via secondary activation of silent synapses or polysynaptic pathways associated with A fibers[25,26,27].

It has been shown previously that following peripheral nerve injury and inflammation, SGCs are activated by the neurons they are enveloping[1,28]. In turn, the activated SGCs release signaling molecules, such as ATP and the cytokines TNFa and IL-1b, causing enhancement of the excitability of the neurons they are enveloping, and adjacent neurons via SGC-neuron and SGC-SGC communication, and thus contributing to the development of pathologic pain[1,7].

We observed significant increase of glutamate level in trigeminal SGCs that envelop neurons of all sizes following peripheral nerve injury, suggesting involvement of SGCs that envelop primary sensory neurons of all types, including nociceptive and mechanosensitive neurons, in the SGC-neuron and SGC-SGC communication following nerve injury. It also raises the possibility, albeit remote, that a mechanism underlying the mechanical allodynia following nerve injury exists in the TG (and DRG) besides that in the brain stem (and the spinal cord).

In rats with nerve injury, the glutamate concentration was higher in SGCs of small neurons than in SGCs of medium or large neurons, suggesting a predominant involvement small (C fiber) neurons and their enveloping SGCs in the neuron-SGC and SGC-SGC communication that contribute to neuronal sensitization and pathologic pain. This complements previous observations of increased expression of substance P (SP), CGRP and nNOS primarily in the small DRG neurons following nerve injury[29,30,31], which can then activate the respective receptors in the SGCs that envelop them[32,33,34]. Expression NMDA glutamate receptors are also reported in the small nociceptive neurons and their enveloping SGCs in the DRG [35,36,37].

When viewed in the light of these results, our findings suggest that glutamate released from the SGCs following nerve injury can intensely activate the nociceptive neurons they envelop, and also neighboring neurons via activation of the SGCs that envelop them. This can contribute to the spread of sensitization to multiple nociceptive and non-nociceptive primary sensory neurons, and ultimately to the development of pathologic pain [1,4,7].

Methods

Animals and tissue preparation

All experimental procedures were approved by the Intramural Animal Care and Use Committee at the Kyungpook National University, and followed the guidelines of the National Institute of Health. All procedures including animal handling, housing and surgical procedures were performed in accordance with the ARRIVE guidelines. Twenty male Sprague-Dawley rats (170–190 g) were used for this study: Eight rats for a behavioral assay for mechanical allodynia following chronic constriction injury of infraorbital nerve (CCI-ION), and then for electron microscopic (EM) immunohistochemistry, six rats for Alizarin-red staining, and six rats for glutamate release assay.

Surgery and behavioral assay for CCI-ION

Rats were anesthetized with intraperitoneal injection of ketamine (40 mg/kg) and xylazine (4mg/kg), and surgery to cause chronic constriction injury of the infraorbital nerve was performed according to the original protocol[38]. Briefly, a one-centimeter incision was made along the gingivo-buccal margin, proximal to the first upper molar. Approximately 5 mm segment of the infraorbital nerve was isolated from the surrounding tissue, and two 5 – 0 chromic gut ligatures were tied loosely around it. The incision was closed with two 4 – 0 silk sutures. In sham animals, the surgery was identical, except that no ligatures were placed around the infraorbital nerve.

For the behavioral assay, rats were habituated for 30 min to a cage in a darkened and noise-free room. Withdrawal responses were measured after 10 trials of 4-second duration in 10-second intervals of constant air-puff pressure, as described previously[39,40]. The response threshold was determined as the air-puff pressure at which the rat responded in 5 of the 10 trials. The cut-off pressure was 40 psi. Statistical analysis was performed using two-way ANOVA and a Bonferroni post-hoc test.

Electron microscopic immunohistochemistry

For EM immunohistochemistry, rats of the sham-operated and CCI-ION groups were anesthetized with intraperitoneal injection of sodium pentobarbital (80 mg/kg) and perfused through the heart with 100 ml heparinized 0.9% saline, followed by 500 ml freshly-prepared fixative, containing 1% paraformaldehyde (PFA) and 2.5% glutaraldehyde in 0.1 M phosphate buffer at pH 7.4 (PB). TGs were dissected out and fixed in the same fixative used for perfusion for an additional 2 hours at 4°C. Sections were cut at 50 μm on a Vibratome, rinsed in PB, and osmicated in 1% osmium tetroxide in PB for 30 min. After that, sections

were dehydrated in graded ethanol, flat-embedded in Durcupan ACM (Fluka, Buchs, Switzerland) between Aclar plastic films (EMS, Hatfield, PA), and cured for 48 hours at 60°C. Small chips containing the ophthalmo-maxillary region of the TG were cut out of the wafers and glued onto blank resin blocks with cyanoacrylate. Thin sections were cut with a diamond knife, mounted on formvar-coated single slot nickel grids, and stained with uranyl acetate and lead citrate. Grids were examined on a Hitachi H7500 electron microscope (Hitachi, Tokyo, Japan) at 80 kV accelerating voltage. Images were captured with Digital Micrograph software driving a cooled CCD camera (SC1000; Gatan, Pleasanton, CA) attached to the microscope, and saved as TIFF files.

Postembedding immunogold staining

Postembedding immunogold staining for glutamate was performed according to the method described previously by us [41,42,43]. Briefly, grids were treated for 6 min in 1% periodic acid, to etch the resin, and for 10 min in 9% sodium periodate, to remove the osmium tetroxide. Grids were then washed in distilled water, transferred to tris-buffered saline containing 0.1% triton X-100 (TBST; pH 7.4) for 10 min, and incubated in 2% human serum albumin (HSA) in TBST for 10 min, to block non-specific binding of the primary antibody. Grids were further incubated with rabbit polyclonal antiserum against glutamate (1:80,000; G6642, Sigma-Aldrich; RRID: AB_259946) in TBST containing 2% HSA for 4 hours at room temperature. To eliminate cross-reactivity, the diluted antiserum was preadsorbed overnight with glutaraldehyde (G)-conjugated amino acids (600 µM glutamine-G, 200 µM β-alanine-G, and 100 µM aspartate-G)[44]. After rinsing in TBST, grids were incubated in goat anti-rabbit IgG antibody coupled to 15 nm gold particles (1:25 in TBST containing 0.05% polyethylene glycol; BioCell, Cardiff, UK; RRID: AB_1769134) for 2 hours at room temperature. After a rinse in distilled water, grids were counterstained with uranyl acetate and lead citrate and examined with the electron microscope, images were captured and saved as above.

The specificity of the immunolabeling was evaluated by omission or replacement of the primary antiserum with normal rabbit serum or by preadsorption of the diluted anti-glutamate serum with 300 µM glutamate-G, which abolished the specific immunostaining. It was also confirmed on "sandwiches" of rat brain macromolecule-glutaraldehyde fixation complexes of GABA, glutamate, taurine, glycine, aspartate and glutamine[45,46], as routinely practiced in our laboratory.

Quantitative analysis

We divided the TG neurons into three groups, based on the size of their somata: small (< 400 µm^2 in cross-sectional area), medium (400–800 µm^2) and large (> 800 µm^2). Twelve TG neurons of each group, together with their enveloping SGCs, in each of 4 rats with CCI-ION, and 4 sham-operated rats, were used. For quantitative analysis of the density of gold particles coding for glutamate (number of gold particles/ µm^2), we gathered data from 80–110 electron micrographs from each of 3 small, 3 medium-sized, and 3 large neuronal somata in each TG. The gold particle density was measured in randomly-selected rectangular areas of 4 µm^2 of the cytoplasm of each neuron (6, 9 and 12 areas per small, medium-sized, and large neurons, respectively, or a total area of 24–48 µm^2 per neuron) and in their enveloping SGCs

(3–12 randomly-selected areas of the cytoplasm, or a total area of 5–50 μm^2 per SGC), using a digitizing tablet and Image J software (NIH, Bethesda, MD). The gold particles over the nucleus and the mitochondria were excluded from analysis. The density of gold particles over extracellular areas was used to normalize for different background density in different sections and different immunohistochemical runs.

Statistical analysis was performed using unpaired Student t-test. The correlation of glutamate density in each neuron to that in its enveloping SGC was studied using Pearson correlation analysis.

Declarations

Data Availability

The datasets generated during and/or analysed during the current study are available from the corresponding author on reasonable request.

Acknowledgments

The authors sincerely thank Dr. Juli Valtschanoff for helpful discussion and careful reading of the manuscript. This work was supported by the National Research Foundation of Korea (NRF) grant funded by the Korea government (MSIT, NRF-2017R1A5A2015391).

Author contribution

All author has full access to all the data in this study and take responsibility for the integrity of the data and the accuracy of the data analysis. Study design: Y.S.K., Y.C.B. Conduction of tracing, immunohitochemistry experiments and electron microscopy: Y.S.C., W.M., J.Y.B., D.H.Y. Analysis and interpretation of data: H.G.K., D.K.A., Y.C.B. Writing of the manuscript: Y.S.K., Y.C.B.

Conflict of interest

The authors declare that they have no conflict of interest.

References

1. Shinoda, M., Kubo, A., Hayashi, Y. & Iwata, K. Peripheral and Central Mechanisms of Persistent Orofacial Pain. *Front. Neurosci.* **13**, 1227. https://doi.org/doi:10.3389/fnins.2019.01227 (2019).
2. Hanani, M. & Spray, D. C. Emerging importance of satellite glia in nervous system function and dysfunction. *Nat. Rev. Neurosci.* **21**, 485-498. https://doi.org/doi:10.1038/s41583-020-0333-z (2020).
3. Chiang, C. Y., Sessle, B. J. & Dostrovsky, J. O. Role of astrocytes in pain. *Neurochem. Res.* **37**, 2419-2431. https://doi.org/10.1007/s11064-012-0801-6 (2012).

4. Laursen, J. C. *et al.* Glutamate dysregulation in the trigeminal ganglion: a novel mechanism for peripheral sensitization of the craniofacial region. *Neuroscience* **256**, 23-35, https://doi.org/10.1016/j.neuroscience.2013.10.009 (2014).
5. Wagner, L. *et al.* Glutamate release from satellite glial cells of the murine trigeminal ganglion. *Neurosci. Lett.* **578**, 143-147. https://doi.org/10.1016/j.neulet.2014.06.047 (2014).
6. da Silva, L. B., Poulsen, J. N., Arendt-Nielsen, L. & Gazerani, P. Botulinum neurotoxin type A modulates vesicular release of glutamate from satellite glial cells. *J. Cell. Mol. Med.* **19**, 1900-1909. https://doi.org/10.1111/jcmm.12562 (2015).
7. Fan, W. *et al.* The role of satellite glial cells in orofacial pain. *J. Neurosci. Res.* **97**, 393-401. https://doi.org/10.1002/jnr.24341 (2019).
8. Mahmoud, S., Gharagozloo, M., Simard, C. & Gris, D. Astrocytes Maintain Glutamate Homeostasis in the CNS by Controlling the Balance between Glutamate Uptake and Release. *Cells* **8**, 184. https://doi.org/10.3390/cells8020184 (2019).
9. Hanani, M. Satellite glial cells in sensory ganglia: from form to function. *Brain. Res. Brain. Res. Rev.* **48**, 457-476. https://doi.org/10.1016/j.brainresrev.2004.09.001 (2005).
10. Le Pichon, C. E. & Chesler, A. T. The functional and anatomical dissection of somatosensory subpopulations using mouse genetics. *Front. Neuroanat* **8**, 21. https://doi.org/10.3389/fnana.2014.00021 (2014).
11. Nascimento, R. S., Santiago, M. F., Marques, S. A., Allodi, S. & Martinez, A. M. Diversity among satellite glial cells in dorsal root ganglia of the rat. *Braz. J. Med. Biol. Res.* **41**, 1011-1017. https://doi.org/10.1590/s0100-879x2008005000051 (2008).
12. Ottersen, O. P. Postembedding immunogold labelling of fixed glutamate: an electron microscopic analysis of the relationship between gold particle density and antigen concentration. *J. Chem. Neuroanat.* **2**, 57-66 (1989).
13. Ottersen, O. P. Quantitative electron microscopic immunocytochemistry of neuroactive amino acids. *Anat. Embryol.* **180**, 1-15. https://doi.org/10.1007/BF00321895 (1989).
14. Cho, Y. S. *et al.* Rat odontoblasts may use glutamate to signal dentin injury. *Neuroscience* **335**, 54-63. https://doi.org/10.1016/j.neuroscience.2016.08.029 (2016).
15. Paik, S. K. *et al.* Distribution of excitatory and inhibitory axon terminals on the rat hypoglossal motoneurons. *Brain. Struct. Funct.* **24**, 1767-1779. https://doi.org/10.1007/s00429-019-01874-0 (2019).
16. Kung, L. H. *et al.* Evidence for glutamate as a neuroglial transmitter within sensory ganglia. *PLoS One* **8**, e68312. https://doi.org/10.1371/journal.pone.0068312 (2013).
17. Hoffman, E. M., Zhang, Z., Schechter, R. & Miller, K. E. Glutaminase Increases in Rat Dorsal Root Ganglion Neurons after Unilateral Adjuvant-Induced Hind Paw Inflammation. *Biomolecules* **6**, 10. https://doi.org/10.3390/biom6010010 (2016).
18. Harper, A. A. & Lawson, S. N. Conduction velocity is related to morphological cell type in rat dorsal root ganglion neurones. *J. Physiol.* **359**, 31-46. https://doi.org/10.1113/jphysiol.1985.sp015573

(1985).

19. Lawson, S. N. & Waddell, P. J. Soma neurofilament immunoreactivity is related to cell size and fibre conduction velocity in rat primary sensory neurons. *J. Physiol.* **435**, 41-63. https://doi.org/10.1113/jphysiol.1991.sp018497 (1991).
20. deGroot, J., Zhou, S. & Carlton, S. M. Peripheral glutamate release in the hindpaw following low and high intensity sciatic stimulation. *Neuroreport* **11**, 497-502. https://doi.org/10.1097/00001756-200002280-00014 (2000).
21. Dmitrieva, N., Rodríguez-Malaver, A. J., Pérez, J. & Hernández, L. Differential release of neurotransmitters from superficial and deep layers of the dorsal horn in response to acute noxious stimulation and inflammation of the rat paw. *Eur. J. Pain* **8**, 245-252. https://doi.org/10.1016/j.ejpain.2003.09.001 (2004).
22. Kumar, N. *et al.* Systemic pregabalin attenuates facial hypersensitivity and noxious stimulus-evoked release of glutamate in medullary dorsal horn in a rodent model of trigeminal neuropathic pain. *Neurochem. Int.* **62**, 831-835. https://doi.org/10.1016/j.neuint.2013.02.022 (2013).
23. Chiang, C. Y. *et al.* Endogenous ATP involvement in mustard-oil-induced central sensitization in trigeminal subnucleus caudalis (medullary dorsal horn). *J. Neurophysiol.* **94**, 1751-1760. https://doi.org/10.1152/jn.00223.2005 (2005).
24. Zhou, C. & Luo, Z. D. Electrophysiological characterization of spinal neuron sensitization by elevated calcium channel alpha-2-delta-1 subunit protein. *Eur. J. Pain* **18**, 649-658. https://doi.org/10.1002/j.1532-2149.2013.00416.x (2014).
25. Devor, M. Ectopic discharge in Abeta afferents as a source of neuropathic pain. *Exp. Brain Res.* **196**, 115-128. https://doi.org/10.1007/s00221-009-1724-6 (2009).
26. Sandkühler, J. Models and mechanisms of hyperalgesia and allodynia. *Physiol. Rev.* **89**, 707-758. https://doi.org/ 10.1152/physrev.00025.2008 (2009).
27. Torsney, C. Inflammatory pain unmasks heterosynaptic facilitation in lamina I neurokinin 1 receptor-expressing neurons in rat spinal cord. *J. Neurosci.* **31**, 5158-5168. https://doi.org/10.1523/JNEUROSCI.6241-10.2011 (2011).
28. Chiang, C. Y., Dostrovsky, J. O., Iwata, K. & Sessle, B. J. Role of glia in orofacial pain. *Neuroscientist* **17**, 303-320. https://doi.org/10.1177/1073858410386801 (2011).
29. Luo, Z. D. *et al.* Neuronal nitric oxide synthase mRNA upregulation in rat sensory neurons after spinal nerve ligation: lack of a role in allodynia development. *J. Neurosci.* **19**, 9201-9208. https://doi.org/10.1523/JNEUROSCI.19-21-09201.1999 (1999).
30. Fukuoka, T. & Noguchi, K. Contribution of the spared primary afferent neurons to the pathomechanisms of neuropathic pain. *Mol. Neurobiol.* **26**, 57-67. https://doi.org/10.1385/MN:26:1:057 (2002).
31. Martin, S. L., Reid, A. J., Verkhratsky, A., Magnaghi, V. & Faroni, A. Gene expression changes in dorsal root ganglia following peripheral nerve injury: roles in inflammation, cell death and nociception. *Neural Regen. Res.* **14**, 939-947. https://doi.org/10.4103/1673-5374.250566 (2019).

32. De Corato, A. *et al.* Trigeminal satellite cells express functional calcitonin gene-related peptide receptors, whose activation enhances interleukin-1β pro-inflammatory effects. *J. Neuroimmunol.* **237**, 39-46. https://doi.org/10.1016/j.jneuroim.2011.05.013 (2011).
33. Goto, T., Iwai, H., Kuramoto, E. & Yamanaka, A. Neuropeptides and ATP signaling in the trigeminal ganglion. *Jpn. Dent. Sci. Rev.* **53**, 117-124. https://doi.org/10.1016/j.jdsr.2017.01.003 (2017).
34. Zhang, Y. *et al.* Activation of mitogen-activated protein kinases in satellite glial cells of the trigeminal ganglion contributes to substance P-mediated inflammatory pain. *Int. J. Oral Sci.* **11**, 24. https://doi.org/10.1038/s41368-019-0055-0 (2019).
35. Castillo, C. *et al.* Satellite glia cells in dorsal root ganglia express functional NMDA receptors. *Neuroscience* **240**, 135-146. https://doi.org/10.1016/j.neuroscience.2013.02.031 (2013).
36. Ferrari, L. F. *et al.* Inflammatory sensitization of nociceptors depends on activation of NMDA receptors in DRG satellite cells. *Proc. Natl. Acad. Sci. U. S. A.* **111**, 18363-18368. https://doi.org/10.1073/pnas.1420601111 (2014).
37. Gong, K., Kung, L. H., Magni, G., Bhargava, A. & Jasmin, L. Increased response to glutamate in small diameter dorsal root ganglion neurons after sciatic nerve injury. *PLoS One* **9**, e95491. https://doi.org/10.1371/journal.pone.0095491 (2014).
38. Imamura, Y., Kawamoto, H. & Nakanishi, O. Characterization of heat-hyperalgesia in an experimental trigeminal neuropathy in rats. *Exp. Brain Res.* **116**, 97–103. https://doi.org/10.1007/pl00005748 (1997).
39. Ahn, D. K. *et al.* Compression of the trigeminal ganglion produces prolonged nociceptive behavior in rats. *Eur. J. Pain* **13**, 568–575. https://doi.org/10.1016/j.ejpain.2008.07.008 (2009).
40. Ahn, D. K. *et al.* Intratrigeminal ganglionic injection of LPA causes neuropathic pain-like behavior and demyelination in rats. *Pain* **146**, 114–120. https://doi.org/10.1016/j.pain.2009.07.012 (2009).
41. Paik, S. K. *et al.* Development of gamma-aminobutyric acid-, glycine-, and glutamate-immunopositive boutons on rat jaw-opening motoneurons. J. Comp. Neurol. **520**, 1212–1226. https://doi.org/10.1002/cne.22771 (2012).
42. Paik, S. K. *et al.* Gamma-Aminobutyric acid-, glycine-, and glutamate-immunopositive boutons on mesencephalic trigeminal neurons that innervate jaw-closing muscle spindles in the rat: ultrastructure and development. *J. Comp. Neurol.* **520**, 3414–3427. https://doi.org/10.1002/cne.23110 (2012).
43. Paik, S. K., Yoshida, A. & Bae, Y. C. Development of γ-aminobutyric acid-, glycine-, and glutamate-immunopositive boutons on the rat genioglossal motoneurons. *Brain Struct. Funct.* **226**, 889-900. https://doi.org/ 10.1007/s00429-021-02216-9 (2021).
44. Ottersen, O. P., Storm-Mathisen, J., Madsen, S., Skumlien, S. & Stromhaug, J. Evaluation of the immunocytochemical method for amino acids. *Med. Biol.* **64**, 147–158 (1986).
45. Ottersen, O. P. Postembedding light- and electron microscopic immunocytochemistry of amino acids: description of a new model system allowing identical conditions for specificity testing and tissue processing. *Exp. Brain Res.* **69**, 167-174. https://doi.org/10.1007/BF00247039 (1987).

46. Paik, S. K. *et al.* Developmental changes in distribution of gamma-aminobutyric acid- and glycine-immunoreactive boutons on rat trigeminal motoneurons. I. Jaw-closing motoneurons. *J. Comp. Neurol.* **503**, 779-789. https://doi.org/10.1002/cne.21423 (2007).

Figures

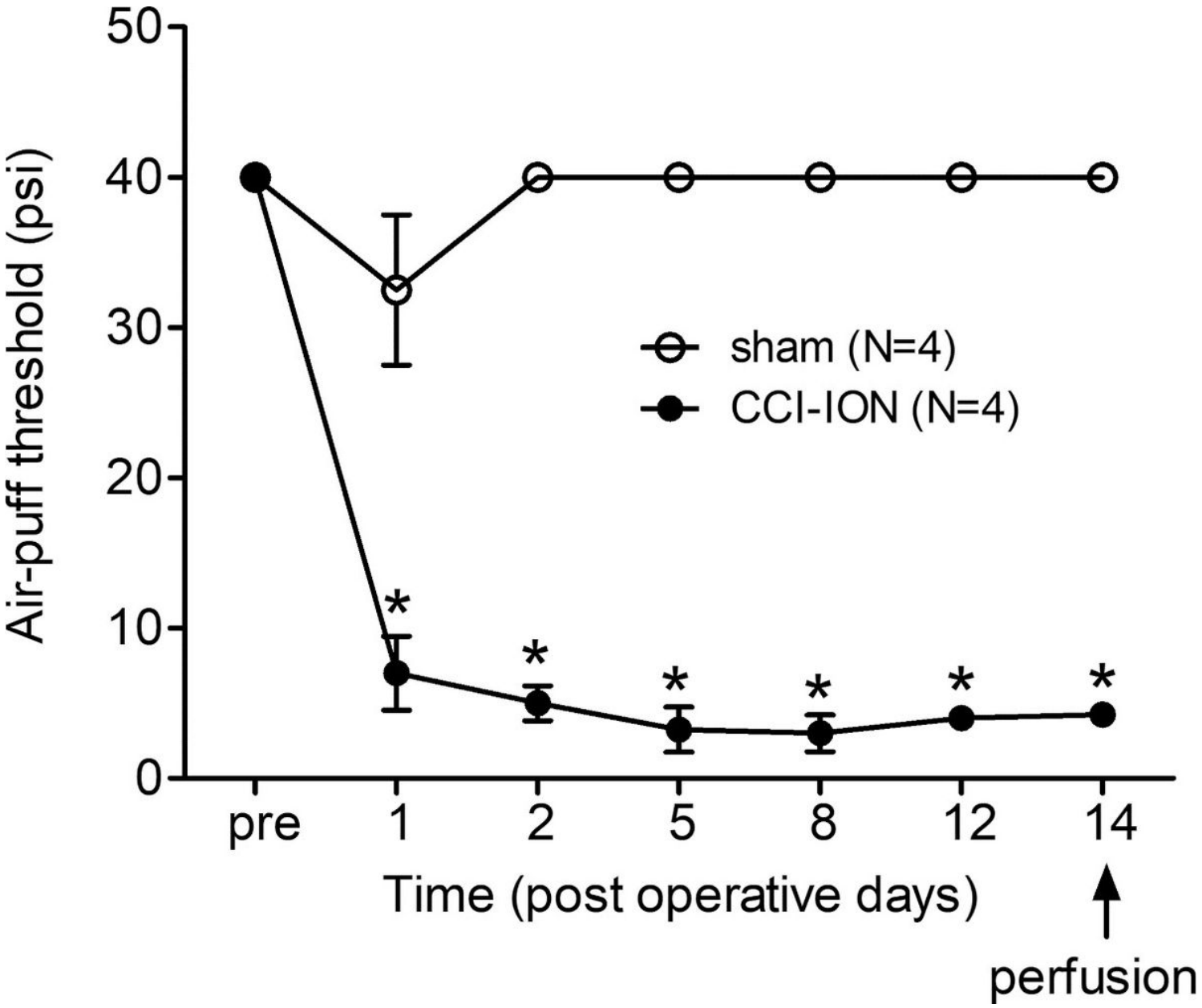

Figure 1

Increased withdrawal response to mechanical stimulation following chronic constriction injury of the infraorbital nerve (CCI-ION) in rats: Air puff-threshold was significantly decreased (Mean ± SD) from day 1 following CCI-ION until day 14, when rats were sacrificed through perfusion for electron microscopic analysis. * P<0.001, sham vs. CCI-ION group, two-way ANOVA, Bonferroni post-hoc analysis.

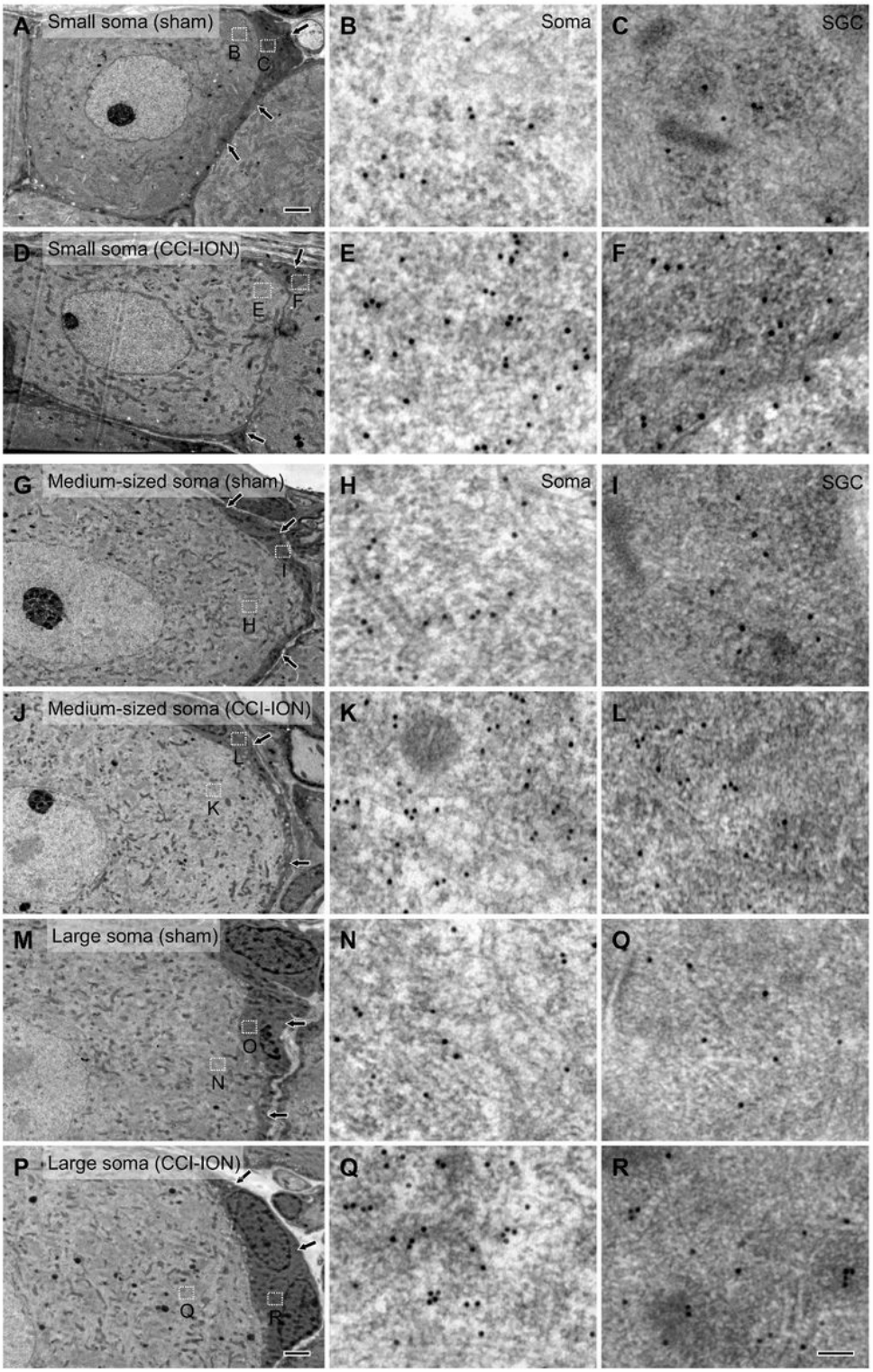

Figure 2

Electron micrographs of the trigeminal ganglion showing immunogold labeling for glutamate in small (A-F), medium-sized (G-L) and large (M-R) neurons and their satellite glial cells (SGCs, arrows) in sham (A-C, G-I and M-O) and CCI-ION (D-F, J-L and P-R) rats; gold particles are denser in the CCI-ION than the sham-operated rats. (B-C, E-F, H-I, K-L, N-O, and Q-R) are enlargements of the boxed areas in the neuron and

SGCs in (A, D, G, J, and M), respectively. Scale bars = 2 μm in (P): (also applies to A, D, G, J and M) and 0.1 μm in (R): (also applies to B, C, E, F, H, I, K, L, N, O and Q).

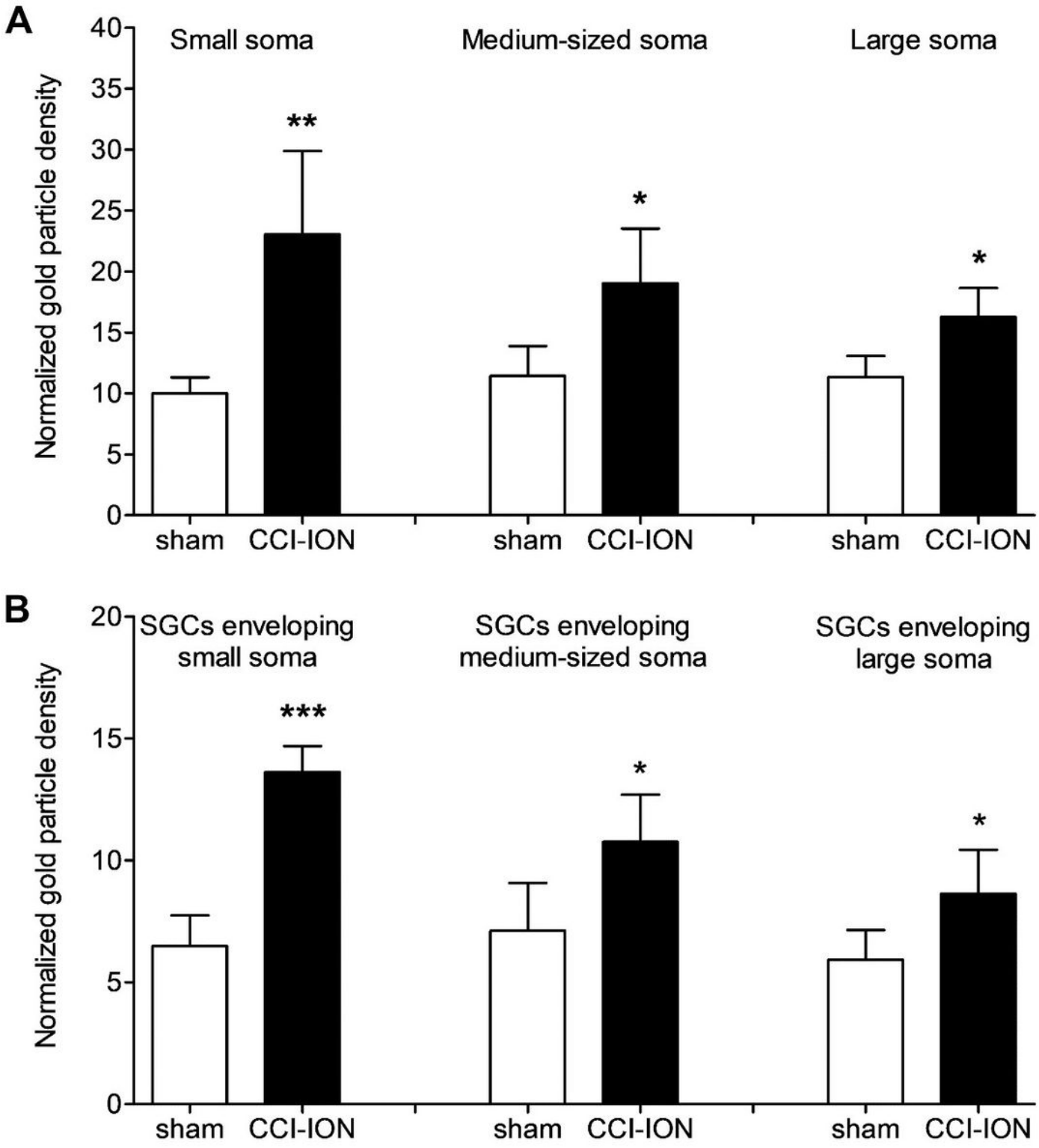

Figure 3

Normalized value (Mean ± SD) of the density of gold particles coding for glutamate in small, medium-sized, and large trigeminal neurons (A) and their satellite glial cells (SGCs, B) in sham-operated and CCI-ION rats. Gold particle density is significantly higher in the CCI-ION rats than sham-operated rats.

Furthermore, gold particle density is higher in the small neurons and their enveloping SGCs than in medium-sized and large neurons and their enveloping SGCs in CCI-ION rats. Normalized value is the gold particle density over the cytoplasm of neurons or SGCs divided by the gold particle density over the same area of extracellular matrix. N= 3 trials in each group. *P<0.05, **P<0.01, ***P<0.001, unpaired t-test.

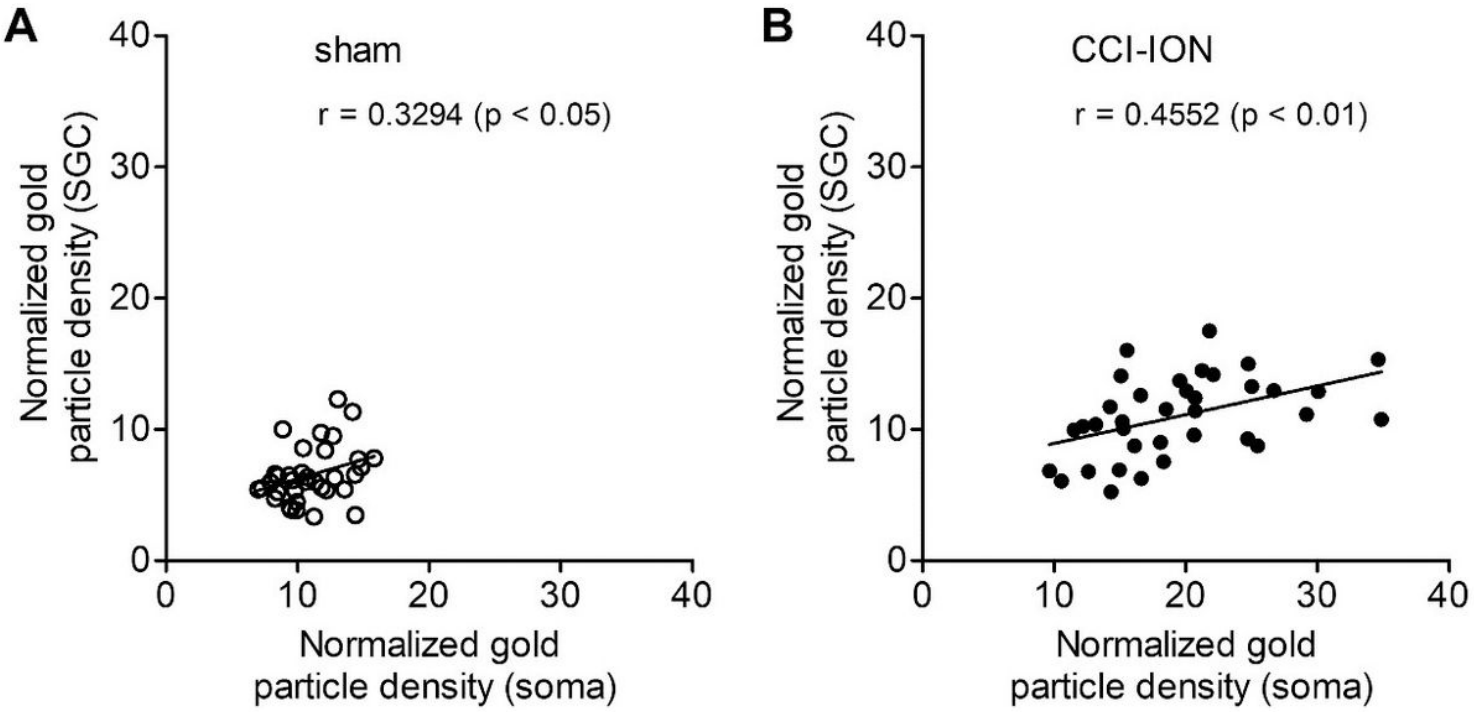

Figure 4

Scatterplots showing positive correlation between the density of gold particles coding for glutamate in trigeminal neurons and that in their enveloping satellite glial cells (SGCs) in the sham-operated (A) and CCI-ION (B) rats; the correlation is stronger in the CCI-ION than in the sham-operated rats.